

## Development of Optimal Thresholding Technique for Shape and Size Detection for Through-the-wall Radar Imaging System

Akhilendra Pratap Singh<sup>#,\*</sup>, Smrity Dwivedi<sup>#</sup>, and Pradip Kumar Jain<sup>#, @</sup>

<sup>#</sup>Indian Institute of Technology, BHU, Varanasi, India

<sup>@</sup>National Institute of Technology, Patna, India

\*E-mail: [apsingh.rs.ece14@itbhu.ac.in](mailto:apsingh.rs.ece14@itbhu.ac.in)

### ABSTRACT

Through-the-wall radar (TWR) images of stationary target behind a wall are subject to strong stationary and non-stationary clutter which obscures the target position and size in the image. Stationary clutters are present due to strong reflection from the wall and non-stationary clutter occurs due to multipath, noise, etc. A lot of work has been reported for mitigating stationary clutter successfully for various real scenarios. However, for mitigating non-stationary clutter various authors have reported their work in this field but any concrete result has not been reported so far. Hence, there is a need for an optimal methodology to mitigate non-stationary clutter in TWR images for achieving a high-quality image representing the target position, shape and its size. Till now it is difficult to achieve shape detection of the target from the TWR system. Therefore, in this paper, a novel optimal thresholding technique is proposed to mitigating non-stationary clutter for further enhancement on shape detection of a target using curve fitting and genetic algorithm. The proposed methodology gives a satisfactory result and can prove to be a powerful technique for minimising clutter.

**Keywords:** Through wall imaging; Shape and size detection; Curve fitting; Statics-based thresholding; TWR imaging system

### 1. INTRODUCTION

Through the wall radar (TWR) is emerging technology which enables us to image targets behind a wall. The challenge which exists is to detect the target from images generated by TWR imaging systems. The TWR images of stationary target behind a wall are subject to stationary and non-stationary clutter which obscures the target image. Thus there is a need a methodology to enhance the detection of the target while mitigating the clutter. The common aim of the detection method is to indicate the presence or absence of targets in the TWR image. The first approach in the detection of a target is to mitigate stationary clutter from strong wall reflection. So far, various researchers have proposed a methodology for mitigating clutter due to the wall. The foremost approach can be based on background subtraction. This approach relies on prior knowledge of the background scene. It gives good results but is not feasible in the real scenario because prior knowledge of the background scene cannot be obtained in a real scenario. As a result, in order to address this problem from high wall reflection, some other approaches have been proposed such as statistical methods<sup>1,3,4</sup>, spatial filtering<sup>2</sup>, etc. These approaches don't rely on prior knowledge of the background scene.

After mitigating the stationary clutter in TWR image, thresholding is applied to the image to separate target pixels from non-stationary clutter, and thereby further enhance

the image quality for the enhancement of target detection. Various researchers have reported about choosing an optimum threshold for mitigating non-stationary clutter. Debes<sup>5,6</sup>, *et al.* have used statistical detectors based on likelihood ratio tests for detection of stationary targets in TWR images. In this test, a Neyman-Pearson criterion was formulated for choosing a threshold for separating targets pixels in TWR images while controlling false alarm rate. But this test has been requiring a priory probability density functions (pdfs) for the TWR images. Since information about pdf cannot be obtained a priory, therefore Debes<sup>5,6</sup>, *et al.* have proposed a methodology which adapts the statistics parameters corresponds to the TWR image statistics for implementation of Neyman-Pearson test. Further, morphological filtering was used to optimise the estimates test parameters<sup>7</sup>. These approaches provide quality images, but they assume a priory probability density functions (pdfs) of targets and clutters in radar images. These assumed pdfs may differ for the various scenarios. Therefore in most cases appropriate pdfs and FAR needs to define a priory every time for both targets and clutter in TWR image, which presents a shortcoming of using likelihood ratio tests detection of the target. To overcome this limitation, there exist some automatic threshold selection techniques. Such techniques use a discriminant criterion by maximising the separability of the resultant classes to select an optimal threshold. However, in most real scenario histograms of TWR image does not exhibit a traceable valley. Therefore it becomes difficult to obtain a concrete result. In lieu of these approaches, an optimal algorithm/methodology has been

proposed for enhancement of detection of a target using curve fitting and genetic algorithm. In the proposed methodology, the fitness function will generate the optimised threshold value based on image statistics of TWR image of the target while controlling accuracy and false alarm in a user-defined constraint. The advantage with the proposed method is that it won't require the assumption of pdf and histogram in each scenario for choosing the optimum threshold.

In order to carry out detection task, an experiment has been carried out to collect C-scan data of different materials of different shape and size. The data were collected by TWR imaging system at a frequency range of 3.5 GHz–5.5 GHz.

## 2. MEASUREMENT SET-UP FOR THROUGH-THE-WALL IMAGING SYSTEM

An SFCW radar has been assembled using Anritsu VNA (MS2037C) and horn antenna working in the frequency range of 3.5-5.5 GHz for the generation of Through-the-wall radar images. In continuous wave radar, cross-range resolution is dependent on the frequency of the signal that requires operation at higher frequencies. On the other hand attenuation of the signal due to the wall also increases at a higher frequency. Thus, there exist a trade-off between resolution and penetration. In the previous article, attenuation due to brick wall is reported as 5 dB/cm at 5 GHz and for concrete wall as 10 dB/cm at 3 GHz<sup>8</sup>. From the above observations, it is inferred that the selection of frequency range up to approximately 5 GHz can be done as attenuation is within acceptable limit<sup>8</sup>. So, we have selected frequency range of 3.95–5.95 GHz for imaging.

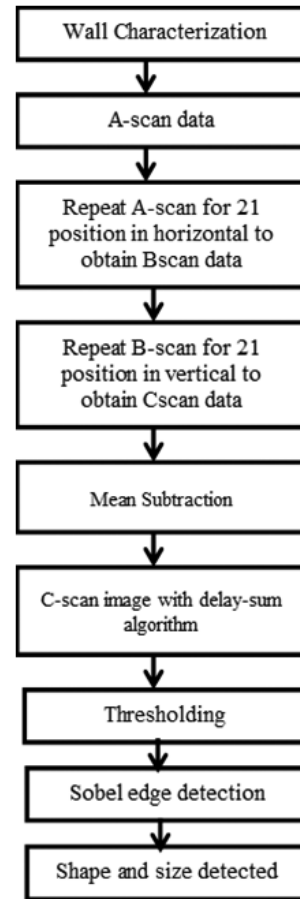
Table 1 shows the typical value of designed SFCW radar parameters for imaging. The antenna is placed on a 2D field scanner which enables the antenna to move in the horizontal direction and vertical direction. The radar is kept at 220 cm from the wall. The target is placed at 122 cm on the other side of the wall. The target is placed on a wooden stand covered by absorbing sheet to minimise any reflection from the stand. Four different triangular, square, circular and rectangular shapes and sizes of wooden and metallic targets are considered. The detail list of the target used for the purpose of target recognition is given in Table 7. In order to capture entire information of the scene behind walls, S-parameter S11 was collected at 21 horizontal and 21 vertical scan points to completely cover the target. The inter-element spacing between each scan point is 5 cm.

**Table 1. Typical values of SFCW Radar parameters**

Radar parameters	Value
Frequency range	3.5 GHz - 5.5 GHz
Bandwidth	2 GHz
Number of frequency points	201
Power transmitted	-3 dbm
Range resolution	7.5 cm
Antenna type	Horn
Beam width	20 degree
Gain	18 dB

## 3. SIGNAL PROCESSING FOR SHAPE AND SIZE DETECTION OF TARGET

Flowchart of different steps applied is shown in Fig. 1. For forming the TWR image of the scene, it is important to know the characteristics of the wall such as dielectric constant, as this may affect the quality of the image.



**Figure 1. Flowchart of signal processing steps.**


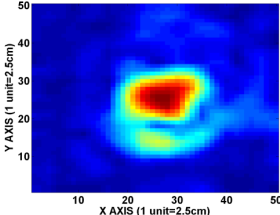

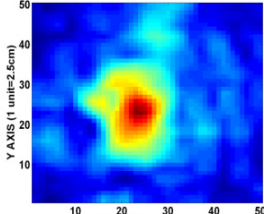

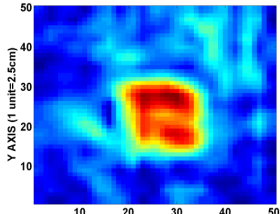

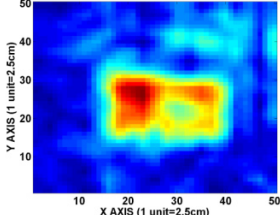
In the present article, the dielectric value of wall for each frequency in the experimental band of 3.95 -5.95 GHz has been estimated in a similar manner as proposed by Muqaibal<sup>9</sup>, *et al.* The averaged value of estimated dielectric in an experimental band of 3.95 -5.95 GHz can be considered as the dielectric value of wall as suggested by Gaikwad<sup>10</sup>, *et al.* Thus, the dielectric value of the wall was found to be 6.4.

The received signal contains reflected signals from the target as well as undesired signals. These undesired signals are present due to reflection from antenna mismatch, and background noise. To remove these undesired signals, average subtraction method is applied as proposed by Verma<sup>1</sup>, *et al.* For this purpose, the mean vector of each B-scan is calculated and further subtracted from its each individual A-scan. After performing the mean subtraction operation on C-scan data, it has been further processed for the formation of through the wall images using delay and sum beam forming as proposed by Ahmad<sup>11</sup>, *et al.* The raw 2-D TWR image (cross range vs height) of the metallic square (Target id-T1), metallic square (Target id-T2), wooden square (Target id-T3), and wooden

rectangle (Target id-T4), target at 0-degree rotation with its actual target shape is as shown in Table 2.

The raw 2D C-scan image may contain unwanted pixels, other than desired target pixels, due to background noise.

**Table 2. Raw 2D C-Scan TWR Image obtained using delay and sum beamforming method on imaging plane along X and Y axis with its actual shape of target id (a) T1 (b) T2 (c) T3(d) T4**

Actual shape of target	Raw 2D C-scan image of target
 Target ID: T1	 Target ID: T1
 Target ID: T2	 Target ID: T2
 Target ID: T3	 Target ID:T3
 Target ID:T4	 Target ID:T4

Therefore, for enhancement of target pixels various image enhancement methods<sup>12</sup> such as spatial maximum filtering, mean filtering, wiener filtering and adaptive median filtering are considered for investigation. Peak to Signal Noise Ratio (PSNR) is calculated to compare their performance of filtering operation. PSNR is calculated from 2D C-scan image and filtered image according to Eqns. (1)-(2).

Mean Square Error (MSE) =

$$\frac{1}{MXN} \sum_{i=1}^N \sum_{j=1}^M (F(i, j) - I(i, j))^2 \quad (1)$$

$$PSNR (dB) = 10 \log \left( \frac{1}{MSE} \right) \quad (2)$$

As shown in Table 3, the PSNR value of the adaptive median filter is higher compare to spatial filtering techniques. This shows that the adaptive median filter gives good results in comparison with other filtering operations. The adaptive median filtered image of considered targets is as shown in Figs. 2(a)-2(d). These pre-processed images are further used for detection.

**Table 3. PSNR (dB) value of various spatial filtering techniques for target id T1, T2, T3, T4**

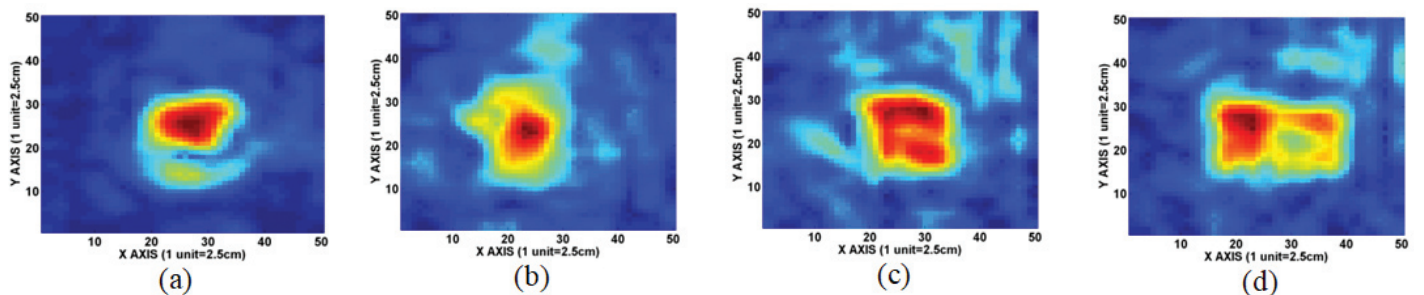
Filtering method	T1	T2	T3	T4
Spatial max	24.89	24.75	25.15	24.04
Mean	37.26	33.86	39.05	33.56
Weiner	40.68	37.28	41.9	36.56
Adaptivemedian	51	44.47	47.22	42.07

### 3.1 Formulation of Statistics based Optimal Thresholding Technique and Implementation

For the considered TWR image of the target, it is observed that reflection from different shape and sizes of wooden and metallic targets have different levels of intensity. For detecting these targets, a proper threshold has to be chosen carefully. Therefore, statistics based thresholding technique has been applied to detect the shape and size of targets. The mean and standard deviation of the image has been calculated and apply the threshold according to given Eqn. (3)

$$Th = \text{mean} + n * \text{standard deviation} \quad (3)$$

Here  $n$  is called a scaling parameter. The image



**Figure 2. Adaptive median filtered image for target id (a) T1, (b) T2, (c) T3, and (d) T4.**

statistics may differ for two 2D C-scan TWR images of a similar scenario therefore, an parameter ‘n’ is included to make equation adaptive in nature (e.g.,  $\mu A \pm p * \sigma D$ ) for thresholding.

The statistics based thresholding technique should give such a threshold which would minimise the false detection of pixels for obtaining the accurate size. Therefore optimum of the value of ‘n’ should be selected based on some parametric analysis so that the desired goal can be achieved. For this purpose, true positive (TP) and false positive (FP) values are computed from 2D C-scan image of target using Eqns. (4)-(5).

$$TP = \frac{\text{True detected target pixels}}{\text{Total no. of target pixels}} \quad (4)$$

$$FP = \frac{\text{False detected target pixels}}{\text{Total pixels} - \text{Total no. of target pixels}} \quad (5)$$

The true positive value gives the accuracy of target pixels detected and false-positive value gives the false detected pixels. For the purpose of formulating a threshold criterion, four randomly selected different targets Id is considered. The total number of pixels of each targets has been calculated using a priory information about target size, cross- range resolution and step size of antenna movement. The sizes of target T1 and T3 are nearly equal to  $(30 \times 30)$  cm which covers approximate  $(12 \times 12 = 144)$  pixels, the size of target T2 is nearly equal to  $(35 \times 35)$  cm which covers approximate  $(14 \times 14)$  pixels and the size of T4 is nearly equal to  $(50 \times 30)$  cm which covers approximate  $(20 \times 12)$  pixels, respectively. The boundary of targets region has been defined using ground truth information about the location of the target and its size. The pixels detected inside the defined boundary of the target region are considered as true detected pixels. If the pixels are detected outside the defined boundary of the target region, then it denotes false detected pixels. The pixels not detected under the defined boundary of target region denote missed pixels point.

The TP and FP value for Target ID T1, T2, T3 and T4 are calculated for values of  $n$  in range of 0 to 5. The plot of TP and FP value of Target ID T1, T2, T3 and T4 for different value of  $n$  is shown in Figs. 3(a) and 3(b). It is observed that TP and FP value decreases with increasing the value of ‘n’. For a certain value of  $n$ , TP remains near the desired true positive value (i.e., 1). On the other side, the FP value also decreases as the value of  $n$  increases. Thus these two parameters show a relation with scaling parameter  $n$ . For formulating an empirical relation of TP and FP with scaling parameter  $n$  a curve-fitting approach is used. After analysing several relations, the following empirical relations are chosen whose coefficient of determination (R2) values found to be greater than 0.9 for both the relations.

$$TP(n) = a1 \exp\left(-0.6 * \left(\frac{-(m+n*s-b1)}{c1}\right)^2\right) \quad (6)$$

$$FP(n) = a2 \exp\left(-0.6 * \left(\frac{-(m+n*s-b2)}{c2}\right)^2\right) \quad (7)$$

where  $m$  and  $s$  are mean and standard deviation. The constants  $a1$ ,  $b1$ ,  $c1$ ,  $a2$ ,  $b2$  and  $c2$  in Eqns. (6)-(7) have been replaced from their average values as shown in Table 3. From Eqns. (6)-(7), it can be observed that if TP is maximised, FP will also be maximised and vice versa. Such type of problem can be

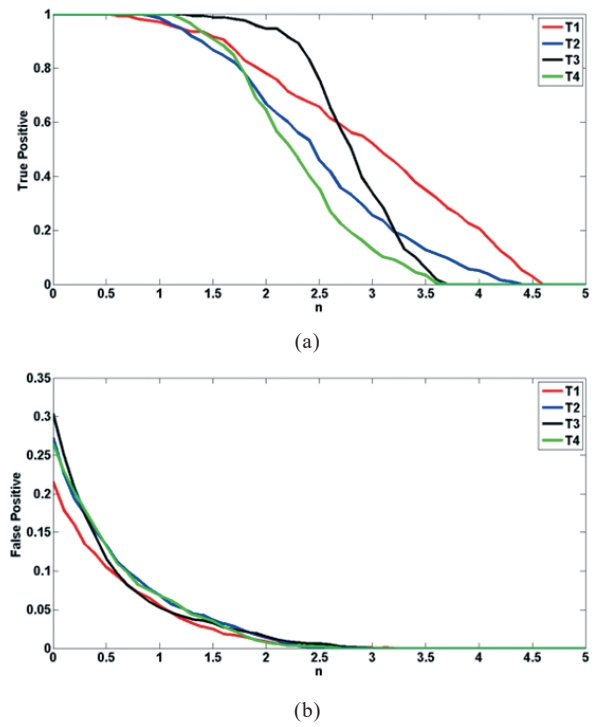


Figure 3. (a) Plot of True positive for different values of  $n$  of concealed targets for target Id T1, T2, T3 and T4 and (b) Plot of False positive for different values of  $n$  of concealed targets for target Id T1, T2, T3 and T4.

addressed using a multi-objective optimisation problem. Here, we have considered a genetic algorithm (GA) based multi-objective optimisation problem to find the optimum value of  $n$  in the range between 0 and 5. GA is an optimisation technique that is globally used for large-scale optimisation problems. We preferred to use GA due to its interesting property such as efficiency, simple programmability and robustness.

For this purpose, function  $Y(n)$  is divided into two functions, i.e.,  $Y1(n)$  and  $Y2(n)$ .  $Y1$  represents the true positive function and  $Y2$  represents a false positive function. Thus  $Y1(n)$  and  $Y2(n)$  can be defined as

Minimising  $Y(n) = [Y1(n), Y2(n)]$ ;  $0 < n < 5$  Such that  $Y1(n) = -TP(n)$  and  $Y2(n) = FP(n)$

Our purpose is to maximise  $TP(n)$  and minimise  $FP(n)$  and thereby find the optimum value of  $n$ . Thus the goal is to be set in such a manner that FP should be lesser than 5 per cent and TP should be greater than the lower boundary 90 per cent. The goal vector is defined as

Goal =  $[-0.9 \ 0.05]$  for fitness function  $Y(n) = [Y1(n), Y2(n)]$ ;

This gives the critical value of  $n$  at which  $TP > 0.9$  and  $FP < 0.05$ . Thus by using the critical value of  $n$  in Eqn. (3), optimal threshold value has been obtained.

#### 4. RESULTS

The developed algorithm is tested with various targets. The following steps are performed for detecting the target using developed algorithm.

Step 1: Mean and Standard deviation is calculated from

the test image.

Step 2: The optimisation goal for GA has been set as per user requirement of TP and FP. Here, we have considered  $FP \leq 5\%$  and  $TP \geq 90\%$ .

Step 3: The optimum value of  $n$  is computed with the help of GA optimisation, using the equation 6 and 7 within the constraint:  $0 < n < 5$ .

Step 4: Using the optimum value of  $n$  in Eqn (3), optimal threshold value is obtained.

The test results of developed algorithm of various targets are as shown in Table 4. The results show that proposed methodology successfully detect targets (target ID: T1, T2, T3, T4) pixels with more than 90% accuracy and also achieved nearly less than 5% of false alarm which was our desired aim of proposed target detection algorithm. Furthermore, the performance of the proposed algorithm for target detection on the basis of true positive (TP) and false positive (FP) value is compared with existing thresholding methods such as maximum entropy- based thresholding method, and Otsu's thresholding method. Table 5 shows the TP and FP values using all four thresholding techniques for target Id T1, T2, T3, and T4. Otsu's method is a well-known global thresholding technique. This method gives a low false positive value for both metallic (Target id T3 and T4) and wooden target (Target id T1 and T2) but provides missed out pixel points for the wooden target (low dielectric targets). Maximum entropy-based thresholding method also gives a low false positive value for metallic targets but it gives missed pixels for the wooden target. Mean based iterative thresholding method provides true target detection for both metallic and wooden targets but it also provides a high false alarm. Proposed thresholding method provides true target detection and low false alarm for each class. It is observed that pre-existing thresholding methods give either false pixels or missed pixel. This occurs due to the wide variation in intensity among target. But proposed statistics-based thresholding method gives good results in comparison with other thresholding methods.

#### 4.1 Validation

The proposed algorithm has been designed to give a threshold value such that FP should be lesser than 5 per cent and TP should be greater than the lower boundary 90 per cent. For validation of developed algorithm, the proposed algorithm is tested with different TWR images of targets which were earlier not used algorithm development and value of true pixel and false pixel is computed. Figs. 4(c), 4(d), 4(i), and 4(j) show the statistics based threshold image of target Id T11, T12, T13 and T14 which are independent data sets and never used earlier for developing the algorithm. Table 6 shows the TP and FP value using the proposed adaptive statistical algorithm for the targets: T11, T12, T13 and T14. The value

**Table 4. Constant value of TP and FP with its R2 for considered targets**

Target ID	a1	b1	c1	R2	a2	b2	c2	R2
T1	1.012	0.2786	0.3775	0.98	5.615	-0.8299	0.4162	99.8
T2	1.033	0.3416	0.2791	0.99	5.611	-0.8297	0.4161	99.8
T3	1.11	0.4673	0.2923	0.95	2369	-2.125	0.6142	99.2
T4	1.07	0.3921	0.2702	0.99	6.339	-0.8051	0.4535	99.7
T5	1.052	0.3708	0.328	0.98	3192	-2.497	0.6714	98.3
T6	0.9652	0.2505	0.3243	0.99	2506	-3.038	0.8121	98
T7	1.095	0.4388	-0.2917	0.95	3002	-1.917	0.5528	98.94
T8	1.03	0.3335	-0.3452	0.98	3225	-3.095	0.8235	92.7
T9	1.05	0.3443	0.3576	0.97	3409	-2.906	0.765	96.6
T10	1.028	0.2701	0.367	0.99	106	-1.209	0.4131	99.4
Average	1.0445	0.3488	0.1959		1782.6	-1.92517	0.59379	

**Table 5. Comparison of thresholding techniques based on TP and FP for target Id T1, T2, T3, T4**

Thresholding methods	True positive				False positive			
	T1	T2	T3	T4	T1	T2	T3	T4
Otsu	0.83	0.81	0.99	0.91	0.01	0.03	0.04	0.03
Entropy	0.80	0.85	0.98	0.96	0.01	0.03	0.03	0.04
Mean	1	1	1	1	0.1	0.2	0.2	0.2
Statistical	0.95	0.95	1	0.98	0.04	0.05	0.04	0.05

**Table 6. Values of scaling parameter  $n$  for unknown targets Id with TP and FP**

Target ID	Mean	Std	$n$	TP	FP
T11	0.2194	0.2230	1.4	1	0.09
T12	0.2338	0.2326	1.3	0.91	0.02
T13	0.2357	0.1817	1.1	0.92	0.03
T14	0.1830	0.2178	0.9	0.91	0.07

of the true pixel and the false pixel of test targets is as shown in Table 6. The results show that proposed algorithm detects target pixels with more than 90 per cent accuracy, which was our desired aim of the proposed target detection methodology and also achieved nearly less than 5 per cent of false alarm. The no. of pixels detected in the target region for targets T11, T12, T13 and T14 are 245, 333, 321, and 306 respectively. This detection can provide vital information about the size of the target. Figs. 4(e), 4(f), 4(k), & 4(l) show the detected shape of target T11, T12, T13 and T14 using Sobel edge detector. Thus it can be observed that the performance of the developed image statistics based detection algorithm for detection of target shape and size on different types of the target shows its adaptive nature.

## 5. CONCLUSIONS

An active SFCW based TWR imaging system was ingeniously designed to illuminate the scene behind a wall at a frequency range of 3.5-5.5 GHz. An adaptive statistics based target shape and size detection algorithm in TWR images was formulated using curve fitting and genetic algorithm based multi-objective optimisation. The proposed target

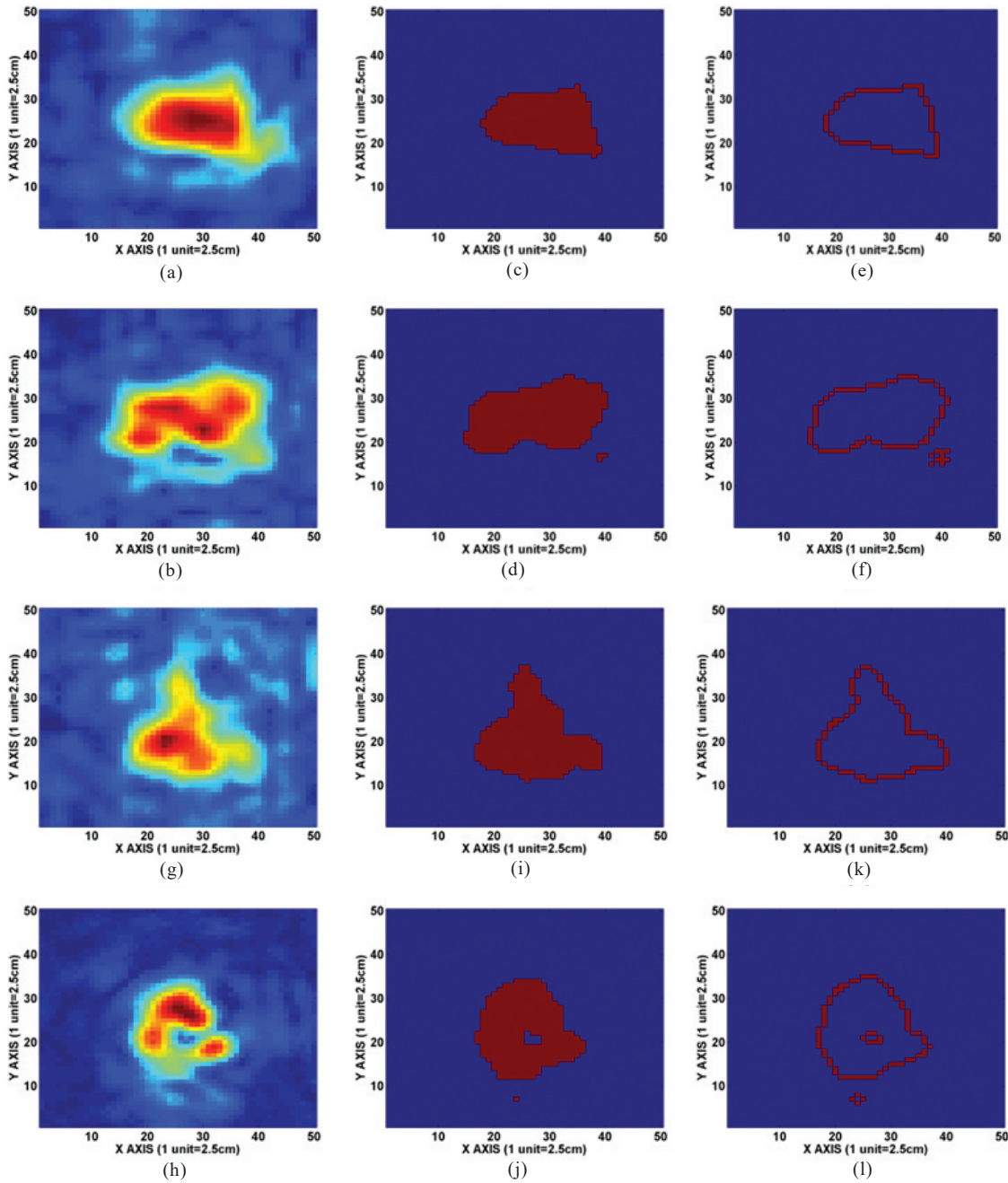


Figure 4. (a) Raw 2D C-scan image of target T11, (b) Raw 2D C-scan image of target T12, (c) 2D C-scan image of target T11 after proposed thresholding technique, (d) 2D C-scan image of target T12 after proposed thresholding technique, (e) 2D C-scan image of target T11 after Sobel edge detection, (f) 2D C-scan image of target T12 after Sobel edge detection, (g) Raw 2D C-scan image of target T13, (h) Raw 2D C-scan image of target T14, (i) 2D C-scan image of target T13 after proposed thresholding technique, (j) 2D C-scan image of target T14 after Sobel edge detection, (k) 2D C-scan image of target T13 after Sobel edge detection, (l) 2D C-scan image of target T14 after Sobel edge detection.

detection algorithm's capability was tested and validated with TWR images of the wooden and metallic target of different shape and size. It is found that based on statistics of TWR image of the target, the fitness function provides an optimal threshold value while maintaining the user-defined constraints of accuracy and false alarm. The results showed that the proposed algorithm detects target pixels with more than 90% accuracy, which was our desired aim of the proposed target detection methodology and also achieved nearly less than 5% of false alarm. The good accuracy of the

proposed algorithm shows that it can be implemented as a generalised.

## REFERENCES

1. Verma, P.K.; Gaikwad, A.N.; Singh, D. & Nigam, M.J. Analysis of clutter reduction techniques for through wall imaging in UWB range. *Progress In Electromagnetics Research*, 2009, **17**, 29-48. doi:10.2528/PIERB09060903.
2. Yoon, Y.S. & Amin, M.G. Spatial filtering for wall-clutter

- mitigation in through-the-wall radar imaging. *IEEE Trans. Geosci. Remote Sensing*, 2009, **47**(9), 3192-3208.  
doi: 10.1109/TGRS.2009.2019728.
3. Gaikwad, A.N.; Singh, D. & Nigam, M.J. Application of clutter reduction techniques for detection of metallic and low dielectric target behind the brick wall by stepped frequency continuous wave radar in ultra-wideband range. *IET Radar, Sonar Navigation*, 2011, **5**(4), 416-425.  
doi: 10.1049/iet-rsn.2010.0059.
  4. Tivive, F. H.C.; Bouzardoum, A. & Amin, M.G. A subspace projection approach for wall clutter mitigation in through-the-wall radar imaging. *IEEE Trans. Geosci. Remote Sensing*, 2014, **53**(4), 2108-2122.  
doi: 10.1109/TGRS.2014.2355211.
  5. Debes, C.; Amin, M.G. & Zoubir, A. M. Target detection in single-and multiple-view through-the-wall radar imaging. *IEEE Trans. Geosci. Remote Sensing*, 2009, **47**(5), 1349-1361.  
doi: 10.1109/TGRS.2009.2013460.
  6. Debes, C.; Riedler, J.; Amin, M. G. & Zoubir, A. M. Iterative target detection approach for through-the-wall radar imaging. *In IEEE International Conference on Acoustics, Speech and Signal Processing*, 2009.  
doi: 10.1109/ICASSP.2009.4960270.
  7. Debes, C.; Riedler, J.; Zoubir, A.M. & Amin, M. G. Adaptive target detection with application to through-the-wall radar imaging. *IEEE Trans. Signal Proc.*, 2010, **58**(11), 5572-5583.  
doi: 10.1109/TSP.2010.2063027.
  8. Frazier, L.M. Surveillance through walls and other opaque materials. *IEEE Aerospace Electron. Sys. Magazine*, 1996, **11**(10), 6-9.  
doi: 10.1109/62.538794.
  9. Muqaibel, A.H. & Safaai-Jazi, A. A new formulation for characterization of materials based on measured insertion transfer function. *IEEE Trans. Microwave Theory Techni.*, 2003, **51**(8), 1946-1951.  
doi: 10.1109/TMTT.2003.815274.
  10. Chandra, R.; Gaikwad, A.N.; Singh, D. & Nigam, M.J. An approach to remove the clutter and detect the target for ultra-wideband through-wall imaging. *J. Geophys. Eng.*, 2008, **5**(4), 412-419.  
doi: 10.1088/1742-2132/5/4/005.
  11. Ahmad, F.; Zhang, Y. & Amin, M. G. Three-dimensional wideband beamforming for imaging through a single wall. *IEEE Geosci. Remote Sensing Lett.*, 2008, **5**(2), 176-179.  
doi: 10.1109/LGRS.2008.915742.
  12. Gonzalez, R.C. & Woods, R.E. Digital image processing. Pearson Education, 2007.

## CONTRIBUTORS

**Mr. Akhilendra Pratap Singh** received MTech (Digital Communication) from ABV Indian Institute of Information Technology and Management, Gwalior, M.P, India. Presently, he is pursuing PhD at Department of Electronics, Indian Institute of Technology (Banaras Hindu University), Varanasi, India. He works in the area of through-the-wall imaging radar.

Contribution in the current study: He conceived the idea of presented research work and developed the algorithm, performed experiments to acquire the data, carried out analysis and interpretation of the data and finally drafted the manuscript.

**Dr Smrity Dwivedi** received PhD in electronics engineering from Indian Institute of Technology (Banaras Hindu University), Varanasi, India. Presently, she is an Assistant Professor in Department of Electronics, Indian Institute of Technology (Banaras Hindu University), Varanasi, India. She has more than 20 paper to her credit published at various global platforms. Her research interest includes high power microwave devices and circuits.

Contribution in the current study: She critically revised the manuscript.

**Dr Pradip Kumar Jain** received PhD in electronics engineering from Institute of Technology, Banaras Hindu University (now IIT (BHU)), Varanasi, India. Presently, he is Director of National Institute of Technology, Patna. He has vast experience of R&D in the area of RF and Communication engineering, microwave/ millimeter wave devices and circuits, high power microwave electron-beam devices. He has been actively engaged in collaborative research with national laboratories in this area.

Contribution in the current study: He supervised the present research work and helped in manuscript drafting.

## APPENDIX

**Table 7. List of target samples used for purpose of training and validation of target detection.**

Target I/D	Shape	Size (length x height) (cm)	Orientation	Material
T1	Square	30 x 30	0	Metal
T2	Square	35 x 35	0	Metal
T3	Square	30 x 30	0	Wood
T4	Rectangle	50 x 30	0	Wood
T5	Square	35 x 35	0	Wood
T6	Rectangle	55 x 35	0	Metal
T7	Circle	Dia= 30	0	Wood
T8	Circle	Dia= 35	0	Wood
T9	Circle	Dia= 30	0	Metal
T10	Circle	Dia= 35	0	Metal
T11	Rectangle	50 x 30	0	Metal
T12	Rectangle	55 x 35	0	Wood
T13	Triangle	50 x 43	0	Wood
T14	Triangle	50 x 43	0	Metal